Electronic Supplementary Material (ESI) for Journal of Materials Chemistry C.

Multiscale Simulation for Exploring Photo-Chemical Processes to Mitigate the Critical Dimension Variability of Contact Hole in EUV Lithography

Sungwoo Park[†,a], Hyungwoo Lee[†,a], Muyoung Kim[a,b], Taegyeom Kim[a], Byunghoon Lee[c], and Maenghyo Cho[*,a,b]

[a]*Division of Multiscale Mechanical Design, School of Mechanical and Aerospace Engineering, Seoul National University, Seoul, Republic of Korea*

[b]*Institute of Advanced Machines and Design, Seoul National University, Seoul, Republic of Korea*

[c]*Mask Development Team, Samsung Electronics CO., Ltd., Suwon, Gyeonggi-do, Republic of Korea*

[†]*These authors contributed equally.*

- **Acid-base diffusion and neutralization coupled with acid-catalyzed deprotection**

We mapped the generated acid/base location data which is following the distribution characteristics of existing L&S into the FDM unit cell. The normalized acid and base concentration were quantified by measuring the distance between each node and the adjacent acid/base site in the FDM model, which utilized a Boltzmann factor in terms of the LJ-fitted interaction energy of reactants (acid-base and acid-tBOCSt)[1]. The derived concentrations were assigned to the nodes as the initial concentrations at PEB time t=0 according to the measured distance (*A* and *Q* in eq (S1)–(S3)).

The methodology for reproducing these acid-base diffusion and neutralization coupled with deprotection follows our previous study[1]. The governing equations are based on Fick's 2nd law and Arrhenius equation as follows:

$$\frac{\partial}{\partial t}(A) = \nabla \bullet (D_A \nabla \bullet A) - k_{quen} AQ \tag{S1}$$

$$\frac{\partial}{\partial t}(Q) = \nabla \bullet (D_Q \nabla \bullet Q) - k_{quen} AQ \tag{S2}$$

$$\frac{\partial}{\partial t}(R_{tBOCSt}) = -k_p A_{pro} R_{tBOCSt} \tag{S3}$$

where A and Q are the acid and base concentrations at each node, D_A and D_Q are the diffusivities for acid and base (5.6nm^2/s and 13.2nm^2/s), k_{quen} is the acid-base neutralization rate coefficient, and A_{pro} and R_{tBOCSt} are the normalized local acid concentration at the location of the protecting group, and the protection ratio with a value between 0 and 1, respectively. The deprotection rate coefficient (k_p = 3.37 s^{-1}) at 363K was derived from our previous DFT calculation[2].

On the basis of the constructed FDM model, with the mapped geometries of tBOCSt groups and acid/base local concentration, acid/base diffusion was implemented following eq (S1) and (S2), reducing the spatial gradient of the concentration contour with an increase of the PEB time. Acid-base neutralization, called quenching reaction, was applied by the third term in eq (S1) and (S2) ($-k_{quen}AQ$), which was replaced by following assumption considering time- and cost-efficiency[1]:

$$A^t = \begin{pmatrix} A^t - Q^t & ;Q^t \le A^t \\ 0 & ;A^t \le Q^t \end{pmatrix} \tag{S4}$$

$$Q^t = \begin{pmatrix} Q^t - A^t & ;A^t \le Q^t \\ 0 & ;Q^t \le A^t \end{pmatrix} \tag{S5}$$

After the time-evolutional acid/base diffusion during PEB time (0–60s) was calculated, the local acid concentration (A_{pro}) at the exact position of tBOCSt group as a function of time was derived by trilinear interpolation of the adjacent 8 node's acid (A) as shown in Figure S1. The interpolated acid concentration (A_{pro}) influences the protection ratio of the corresponding tBOCSt group by the first-order reaction shown in eq (S3).

These coupled differential equations were solved by an explicit forward time-centered space (FTCS) method because of its faster convergence than the implicit method. The periodic boundary conditions in the x, y, and z directions on the outer surface of the unit cell was applied to the FDM simulation, which is same condition to that of the CG simulation environment.

- **Protection ratio of the polymer chain**

The solubility of the PR polymer chain is switched from a hydrophobic to a hydrophilic state as the deprotection of its pendant groups progresses. Using the time-evolutional protection ratio of each tBOCSt group (R_{tBOCSt}) obtained from eq. S3 above, the entire protection ratio of the polymer chain (R_{chain}) was derived as follows:

$$R_{chain} = \left(\sum_{m=1}^{N_P} R_{tBOCSt,\,m} + \sum_{n=1}^{N_D} R_{HOSt,n} \right) \Big/ \left(N_P + N_D \right) \quad \text{(S6)}$$

where N_P and N_D represent the number of initial tBOCSt groups (N_P = 12) and HOSt groups (N_D = 15) in a polymer chain, respectively. $R_{tBOCSt,m}$ and $R_{HOSt,n}$ indicates the protection ratio of the mth tBOCSt and nth HOSt group of the corresponding polymer chain (derived from eq. S3), respectively. (Initial protection ratio of tBOCSt group is 1 (hydrophobic), and the ratio will decrease as deprotection progresses by acid during PEB process. In addition, initial protection ratio of HOSt group is 0 (hydrophilic), and the ratio does not change during PEB because acids only react with tBOCSt group. Therefore, in eq. S6, $\sum_{n=1}^{N_D} R_{HOSt,n}$ is equal to 0.)

According to the calculated protection ratio of each PR polymer chain above (R_{chain}), a polymer chain with a protection ratio less than the conversion threshold $(0.2)^3$ was

determined as a dissoluble polymer chain (solubility switch: hydrophobic → hydrophilic).

- **Supplementary Figures**

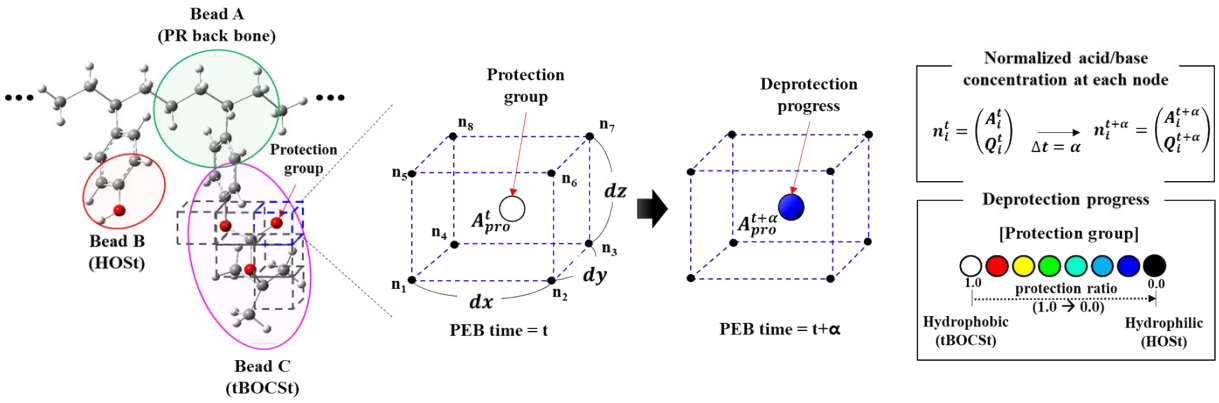

Figure S1. Schematic illustration of mapping pendant group's geometry in CG model into FDM unit cell (space step (dx/dy/dz): 0.185nm/0.185nm/0.195nm), and its deprotection progress by acid/base local concentration (A and Q) at each node (n). The local acid concentration (A_{pro}) at the exact position of the protection group is calculated by trilinear interpolation of the neighboring 8 nodes (n_1~n_8).

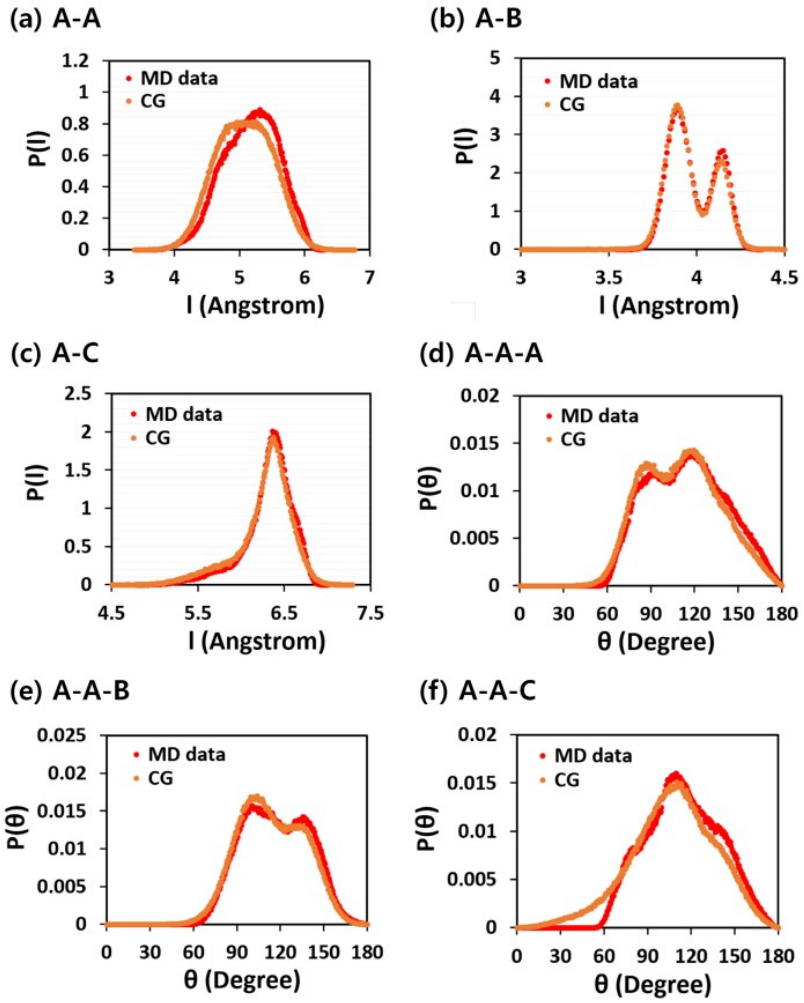

Figure S2. Bond length distributions ($P(l)$) and bending angle distributions ($P(\theta)$) which are obtained from all-atom and coarse-grained models of the PR at 370 K. Red dots: MD data; orange dots: CG data.

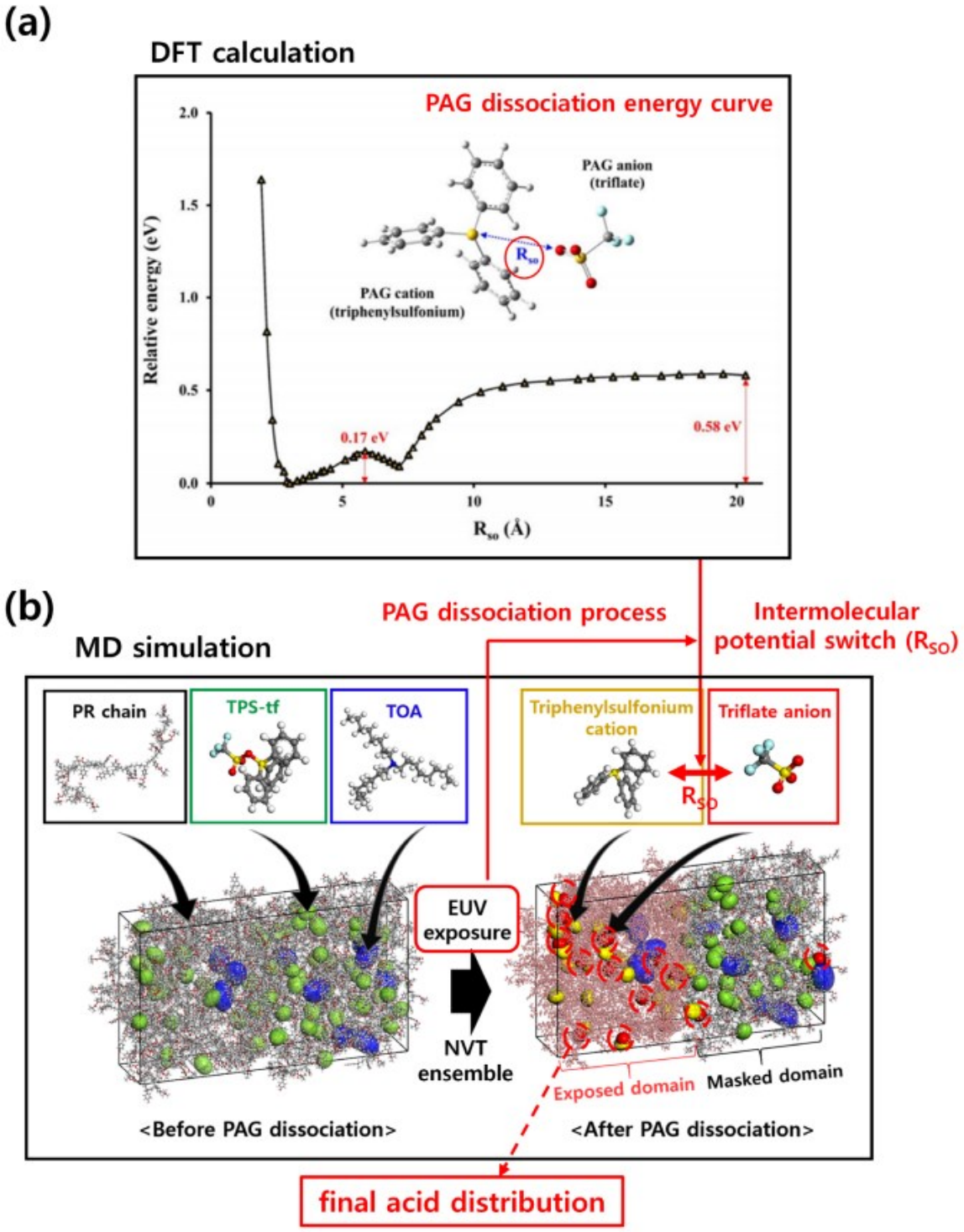

Figure S3. (a) PAG dissociation energy curve from DFT calculation referred from Kim. et al.'s research.[2] R_{so} represents a distance from the oxygen atom (red in the inset) of PAG anion to the sulfur atom (yellow in the inset) of PAG cation. (b) DFT-MD simulation process for PAG dissociation by EUV exposure.[1]

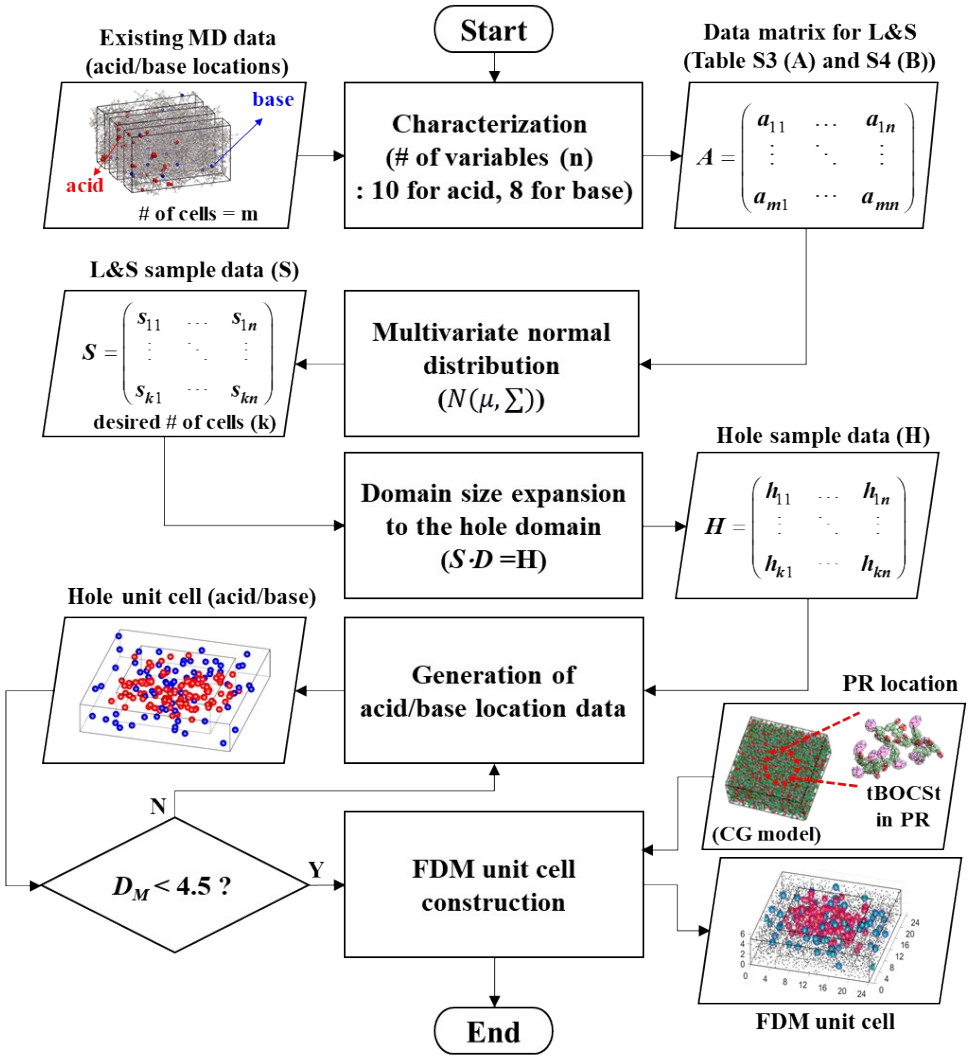

Figure S4. Generation procedure of acid/base location data in the statistical model.

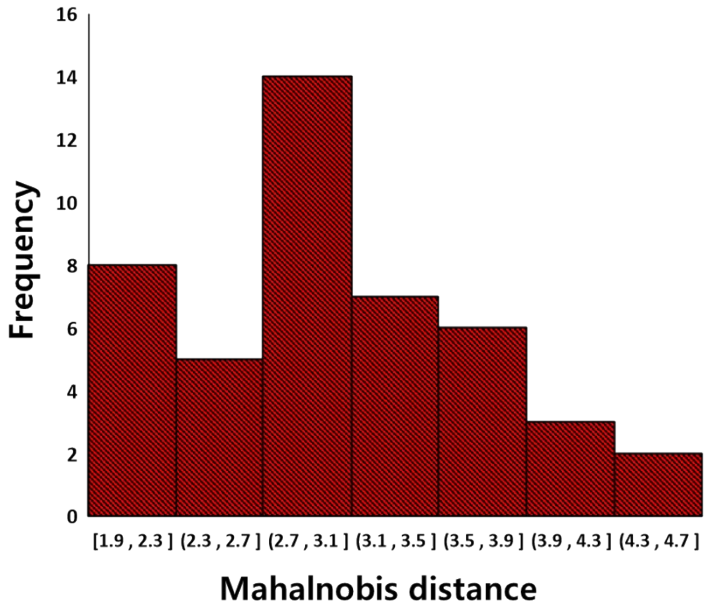

Figure S5. Mahalanobis distance distribution for existing data from MD simulation.

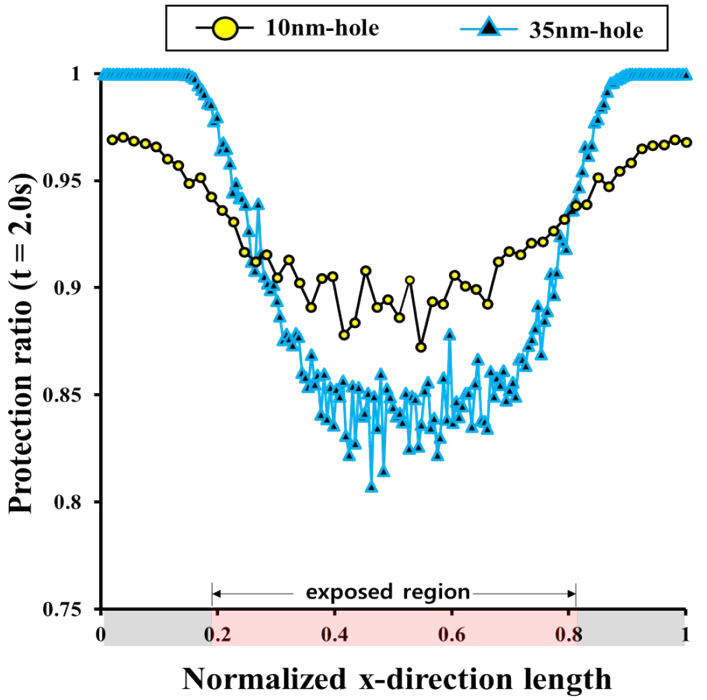

Figure S6. Protection ratio of tBOCSt groups at a PEB time of 2.0 s as a function of normalized x-direction length for 10- and 35 nm-holes. Each point represents an averaged value of the tBOCSt groups within each grid (grid length: 0.3 nm) throughout the x-direction of the entire cell.

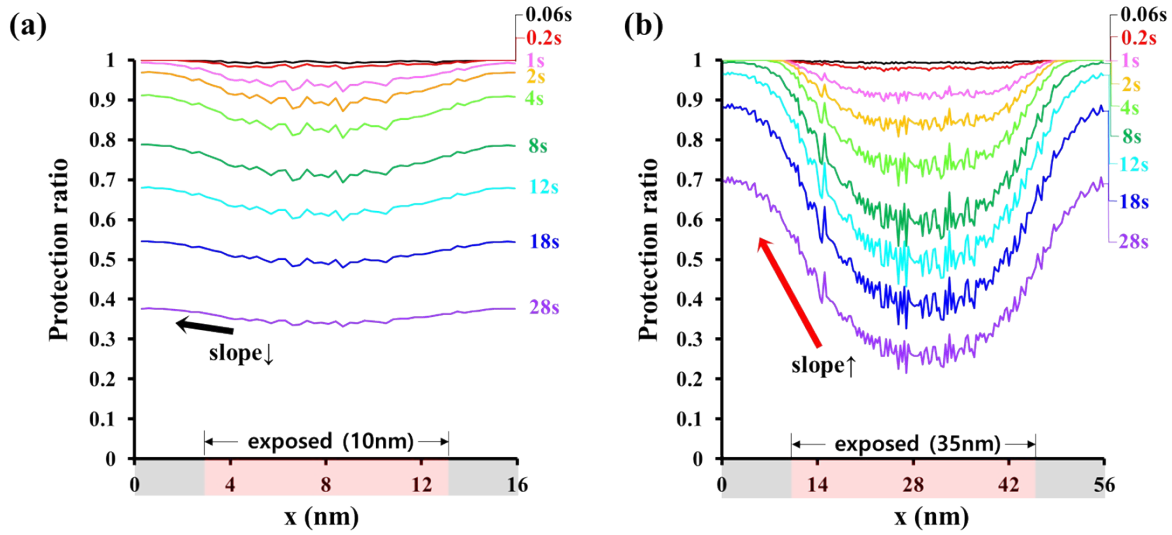

Figure S7. Deprotection progress for the tBOCSt groups along the x axis for a) 10nm-hole and b) 35nm-hole. Each line represents the averaged protection ratio of the individual tBOCSt groups within the corresponding grid (grid length: 0.3nm) throughout the x-direction of the entire FDM unit cell (t = 0.06s–28s).

- **Supplementary Tables**

Table S1. Bond length and bending angle CG potential energy coefficients

Bond length	a_1	b_1 **[Å]**	l_1 **[Å]**	a_2	b_2 **[Å]**	l_2 **[Å]**	a_3	b_3 **[Å]**	l_3 **[Å]**
A-A	0.025	0.446	4.810	0.025	0.415	5.409			
A-B	0.242	0.131	0.100	0.149	0.079	4.137			
A-C	0.006	0.502	5.893	0.011	0.100	6.368	0.036	0.283	6.398
Bending angle	a_1	b_1 [°]	θ_1 [°]	a_2	b_2 [°]	θ_2 [°]	a_3	b_3 [°]	θ_3 [°]
A-A-A	0.010	16.99	84.72	0.013	21.03	118.1	0.001	5.584	143.1
A-A-B	0.016	22.37	102.6	0.020	19.68	141.4			
A-A-C	0.017	41.21	118.3	-0.003	11.56	128.6	0.006	25.67	154.1
	a_4	b_4 [°]	θ_4 [°]						
A-A-A	0.014	33.20	161.0						

Table S2. Variables representing the characteristics of base distribution. (see Figure 5)

No.	**Variables**	**Description**
1-3	x_m, y_m, z_m	average of particle's 3D position (x_j, y_j, and z_j)(j=1, …, N*)
4-6	σ_x, σ_y, σ_z	standard deviation of particle's position
7	ρ	average number of bases in each cluster
8	d	average distance of the bases in the cluster

*N: the number of bases in the unit cell

Table S3 The characteristic data of acid distribution in the reference group for line & space pattern (matrix **A**) from previous MD results (**A** = ($\mathbf{A}_n$)(n=1,…,10), $\mathbf{A}_n$ = (a_{1n}, a_{2n},…, a_{45n})^T)

Cell	$x_{m,a}$ (A_1)	$y_{m,a}$ (A_2)	$z_{m,a}$ (A_3)	$\sigma_{x,a}$ (A_4)	$\sigma_{y,a}$ (A_5)	$\sigma_{z,a}$ (A_6)	N_a^* (A_7)	M_a^{**} (A_8)	ρ_a^{***} (A_9)	d_a^{****} (A_{10})
1	-0.340	-1.105	-0.281	2.493	2.241	0.760	31	2	4.903	0.406
2	-0.073	-0.275	0.704	1.991	2.459	0.789	28	1	2.857	0.332
3	-0.083	0.066	-0.256	2.669	2.235	0.970	25	4	0.880	0.287
4	-0.849	-0.352	0.267	2.491	1.809	1.091	29	6	4.207	0.486
5	-0.403	0.829	-0.093	2.082	2.382	0.750	36	3	4.333	0.361
6	-0.325	-0.593	0.012	2.423	2.641	0.678	29	3	2.621	0.260
7	-0.250	-0.238	0.042	2.159	1.846	1.023	31	1	3.871	0.499
8	-0.794	0.247	0.287	2.197	2.070	1.040	25	3	2.160	0.339
9	-0.364	-1.621	0.108	2.319	2.291	0.944	37	0	4.649	0.331
10	0.169	1.563	-0.152	2.759	2.235	0.658	31	4	2.194	0.305
11	-0.039	-0.361	-0.384	2.083	2.320	0.603	33	2	3.455	0.425
12	0.127	-0.124	-0.062	2.240	2.484	0.852	36	1	3.444	0.411
13	-0.102	-1.071	0.319	2.057	2.169	1.015	34	3	3.471	0.448
14	-0.432	-0.063	-0.025	2.136	2.643	0.982	30	3	2.267	0.311
15	0.411	-0.115	-0.376	2.042	2.204	0.791	29	0	2.345	0.451
16	0.165	-0.510	0.068	2.338	2.686	0.895	32	5	3.438	0.508
17	-0.080	0.023	-0.084	1.946	2.675	0.776	37	0	2.000	0.583
18	0.344	0.112	-0.247	1.864	2.601	0.891	30	2	2.200	0.389
19	0.749	0.247	-0.356	2.249	2.309	0.793	28	0	2.000	0.458
20	0.475	0.614	0.006	2.207	2.048	0.854	35	4	2.914	0.367
21	0.435	-0.921	0.001	2.167	2.695	1.022	29	1	1.310	0.384
22	-0.433	-0.011	0.516	1.886	2.451	0.721	33	1	2.788	0.334
23	0.455	0.320	-0.200	2.267	2.202	1.096	38	2	2.316	0.449
24	-1.027	0.708	-0.075	2.511	2.614	1.016	30	1	2.467	0.332
25	0.956	0.838	-0.154	2.359	2.405	0.974	31	2	2.516	0.526
26	0.469	0.355	-0.007	2.272	2.690	0.727	34	2	2.471	0.434
27	-0.335	0.411	0.236	2.105	2.531	1.010	33	1	1.758	0.389
28	-0.077	-0.019	0.224	2.071	2.291	0.763	32	1	2.250	0.352
29	0.227	0.251	-0.245	2.255	2.294	0.975	32	1	1.438	0.358
30	0.726	-0.764	-0.244	2.487	2.914	0.850	31	5	2.258	0.376
31	-0.373	-0.135	-0.251	2.270	2.384	1.012	36	5	3.222	0.410
32	0.540	-0.186	-0.257	2.397	2.246	0.726	33	1	3.212	0.508
33	-0.259	-0.696	-0.026	2.468	2.067	0.829	37	3	2.757	0.416
34	0.124	-0.100	0.349	2.839	2.782	0.891	31	6	1.935	0.415

35	0.763	1.669	0.139	2.113	2.179	1.126	30	3	1.867	0.389
36	0.321	-0.366	0.221	2.205	2.158	0.882	36	3	3.000	0.466
37	0.241	0.214	0.017	2.533	2.003	0.909	27	2	1.259	0.462
38	-0.440	-0.106	-0.195	2.181	2.384	0.926	30	0	2.333	0.304
39	-0.120	0.384	-0.144	2.172	2.914	0.867	27	1	2.000	0.408
40	0.097	-0.421	0.075	1.832	2.209	0.903	32	1	2.375	0.431
41	0.705	-1.073	0.248	2.159	1.970	1.116	28	1	2.000	0.329
42	0.551	-0.800	0.488	1.900	2.290	0.710	25	0	2.800	0.415
43	-0.392	0.237	-0.168	2.117	2.434	1.079	31	2	2.710	0.243
44	0.114	0.580	-0.134	1.843	2.485	0.795	34	1	6.176	0.378
45	0.043	-0.673	-0.205	1.918	1.905	0.883	36	0	1.778	0.458

*: the number of total acids in the cell.

**: the number of initial acids in the masked domain.

***: clustering density (see Figure 5)

****: average distance between a single particle and corresponding adjacent particles within radius r (=1.0 nm) (see Figure 5)

Table S4 The characteristic data of base distribution in the reference group for line & space pattern (matrix **B**) from previous MD results (**B** = ($\mathbf{B}_n$)(n=1,…,8), $\mathbf{B}_n$ = (b_{1n}, b_{2n},…, b_{37n})^T)

Cell	x_m (B_1)	y_m (B_2)	z_m (B_3)	σ_x (B_4)	σ_y (B_5)	σ_z (B_6)	ρ (B_7)	d (B_8)
1	1.130	-0.070	-0.886	3.402	0.757	2.149	0.200	0.131
2	-2.157	-0.026	-0.999	4.082	0.949	1.967	0.000	0.000
3	2.652	-0.090	-0.516	3.614	1.119	1.792	0.000	0.000
4	2.702	-0.426	-0.335	3.535	0.782	1.693	0.000	0.000
5	-1.418	-0.656	1.215	4.234	0.554	2.289	0.000	0.000
6	1.127	0.333	-0.329	3.622	0.472	2.369	0.000	0.000
7	-0.996	-0.091	-1.463	5.251	0.876	1.848	0.000	0.000
8	1.265	1.018	-0.920	4.653	0.480	0.852	0.400	0.270
9	0.321	-0.139	0.331	4.596	1.016	1.795	0.000	0.000
10	-0.900	0.323	0.233	4.927	0.806	2.709	0.200	0.181
11	-0.178	0.010	0.454	4.463	0.898	2.699	0.200	0.148
12	0.180	-0.054	0.251	4.520	0.951	2.237	0.100	0.080
13	-0.203	0.230	-0.264	5.028	1.058	1.935	0.000	0.000
14	-0.421	0.413	0.437	4.746	0.873	2.574	0.300	0.218
15	-0.265	-0.279	-0.409	4.353	0.926	2.191	0.200	0.180
16	-1.207	-0.177	0.082	4.167	1.001	2.316	0.000	0.000

17	1.794	0.000	0.095	3.750	0.960	2.261	0.080	0.063
18	0.228	-0.165	0.195	4.463	0.946	2.247	0.080	0.067
19	-0.600	-0.035	-0.396	4.444	0.886	2.673	0.160	0.106
20	-0.968	0.086	-0.128	4.858	0.961	2.613	0.160	0.150
21	-0.021	-0.056	0.588	3.910	0.895	2.397	0.080	0.060
22	0.042	0.063	0.382	4.639	1.036	2.411	0.320	0.277
23	-0.546	-0.127	0.330	4.390	0.950	2.634	0.160	0.137
24	2.192	0.191	0.711	3.279	1.025	1.991	0.160	0.132
25	-0.073	0.055	-0.579	4.205	0.883	2.678	0.333	0.230
26	-0.678	-0.106	0.072	3.861	1.004	2.811	0.000	0.000
27	-0.370	-0.317	-0.439	4.326	1.043	2.522	0.000	0.000
28	0.610	0.209	-0.851	4.541	0.850	2.451	0.400	0.275
29	0.584	-0.053	0.212	4.596	1.024	2.651	0.267	0.172
30	1.003	0.134	-0.804	4.365	0.891	2.570	0.000	0.000
31	0.424	0.127	0.382	3.767	0.788	2.417	0.200	0.140
32	0.587	0.056	0.325	3.236	0.916	2.362	0.200	0.133
33	0.664	-0.048	0.147	3.791	1.052	2.207	0.000	0.000
34	-1.187	0.122	-0.902	3.760	0.974	2.439	0.400	0.258
35	-0.607	0.286	0.748	4.804	0.977	2.471	0.250	0.175
36	0.331	-0.183	0.281	4.650	0.981	2.477	0.200	0.146
37	1.134	0.032	-0.031	4.910	0.959	2.822	0.350	0.256

Table S5 Averaged chemical gradient ($\partial R_{chain}/\partial x$) at each hole pattern edge interface (min/max)

Target hole size	**10nm-hole**	**15nm-hole**	**20nm-hole**	**25nm-hole**	**35nm-hole**	**halfH10[c]**
at left edge[a] (minimum)	-0.011	-0.019	-0.024	-0.026	-0.035	-0.021
at right edge[b] (maximum)	0.010	0.020	0.023	0.029	0.035	0.020

a: x = 3, 4.5, 6, 7.5, 10.5 nm for 10- and halfH10, 15-, 20-, 25-, and 35nm-hole, respectively.
b: x = 13, 19.5, 26, 32.5, 45.5nm for 10- and halfH10, 15-, 20-, 25-, and 35nm-hole, respectively.
c: halfH10 indicates the same domain as 10nm-hole except diffusivities (Da: 2.8, and Dq: 6.6 nm^2/s)

References

(1) H. Lee, S. Park, M. Kim, J. Moon, B. Lee, M. Cho, Multiscale Simulation of Extreme Ultraviolet Nanolithography: Impact of Acid-Base Reaction on Pattern Roughness. *J. Mater. Chem. C,* 2021, 9, 1183 - 1195

(2) M. Kim, J. Moon, J. Choi, S. Park, B. Lee, M. Cho, Multiscale Simulation Approach on Sub-10 nm Extreme Ultraviolet Photoresist Patterning: Insights from Nanoscale Heterogeneity of Polymer, *Macromolecules*, 2018, 51, 6922-6935.

(3) E. K. Lin, C. L. Soles, D. L. Goldfarb, B. C. Trinque, S. D. Burns, R. L. Jones, J. L. Lenhart, M. Angelopoulos, C. G. Willson and S. K. Satija, Direct measurement of the reaction front in chemically amplified photoresists, *Science*, 2002, 297, 372–375.